Distributed-Phase-Plate Design Using Simulated Annealing Algorithms

Methods of designing phase plates to achieve control of the far-field irradiance distribution for laser-induced plasma experiments have been under study for more than a decade. One important goal of phase-plate design is to generate the desired far-field spatial profile while minimizing wide-angle scattering outside this profile. This article reports a new algorithm that accomplishes this goal.

Many phase-plate designs reported in the literature have used the phase-retrieval algorithm. These designs achieve a good match to the high-order super-Gaussian distribution that is presumed to approximate the ideal far-field spatial profile. However, the resulting phase plates exhibit wide-angle scattering losses due to steep surface slopes near surface vortices and line discontinuities.[1,2] An article in a previous issue of the LLE Review[3] described an improved phase-retrieval procedure that reduces the number of pole discontinuities and thus the energy loss due to scatter. The present article reports a simulated-annealing algorithm that has resulted in a complete elimination of this source of loss.

Using the classical method of phase retrieval, it is not possible to specify arbitrary constraints or to custom design a cost function for a particular application. To achieve lower scatter by using a strictly continuous phase-plate surface, we have investigated simulated annealing because it allows us to invoke specific constraints, to design with arbitrary cost functions, and, potentially, to find the globally optimum solution for a given set of constraints.[4,5] Using simulated annealing we can specify separately the target far-field profile and the cost function. For example, we can design for specific speckle statistics given the constraint of a specified far-field profile. The cost function may be made sufficiently complex to combine with various weights a number of different factors of importance to a given application.

Algorithm

Our implementation of simulated annealing consists of a number of steps. Starting from an initially aberration-free pupil distribution, a smoothed random wavefront of weak magnitude is constructed and added to the pupil. The far-field irradiance is then calculated by diffraction propagation using fast Fourier transform algorithms, and its azimuthal average $f(r)$ is compared with the desired far-field super-Gaussian irradiance envelope

$$I(r) = e^{-2(r/r_0)^M}, \tag{1}$$

where M is the super-Gaussian order, r is the transverse radius in the far field, and r_0 is the characteristic radius of the far-field distribution. A simple cost function S is evaluated from $f(r)$ and $I(r)$ as

$$S = \int_0^\infty [f(r) - I(r)]^2 2\pi r dr. \tag{2}$$

Cost functions calculated in rectangular coordinates tend to over-constrain the design by reducing the speckle. Use of the azimuthal-average profile as in Eq. (2) provides noise averaging of the quasi-speckle pattern in the far field. Various perturbations of the phase plate are then tried, with the cost function reevaluated each time. If the cost function is lower, the perturbation is accepted and the modified phase plate becomes the basis of further trials. If the cost function is higher than that of the previous cycle, the trial perturbation will be accepted if a random number X, which is uniformly distributed between 0 and 1, is less than the simulated annealing probability p, defined as

$$p = e^{-\Delta S/T}, \tag{3}$$

where ΔS is the change in the cost function due to the perturbation and T is a parameter known as the simulated annealing temperature, the analog of the temperature of an annealing oven. Since the initial, aberration-free pupil matches the target profile quite poorly, the initial cost function is high and ΔS is

quite high also; i.e., relatively small perturbations of the phase plate result in relatively large changes in S. The temperature T is lowered over a number of iterations and serves to control the "cooling" rate of the process. A premise of the theory of simulated annealing is that if the process is cooled sufficiently slowly, local minima will be overcome, resulting in convergence to the global optimum.[4,5]

In our illustrative calculations, the diameter of the pupil was 14 cm, and the desired far-field distribution was a super-Gaussian of eighth order and 700-μm diameter. For a laser wavelength of 0.3511 μm there are about 150 speckles across this diameter. The far-field distribution was sampled using an array of 1024 × 1024 points. Although the beamlines of the OMEGA laser are 28 cm in diameter, the smaller 14-cm diameter was used to reduce computation time.

To find a continuous-surface phase plate that best achieves the desired far-field irradiance envelope, the trial perturbation to the phase plate consists of smoothed random surfaces guaranteeing that the sum of the accepted perturbations will also be strictly continuous. Each cycle of the simulated annealing process requires a unique surface perturbation. Smoothed random surface perturbations are constructed by taking a two-dimensional field of real random numbers and smoothing and scaling this distribution to obtain the desired variance and autocorrelation width. These surface perturbations are made unique by choosing a different random seed for each cycle. We have used an autocorrelation diameter of 0.8 cm, giving about 17.5 autocorrelation diameters over the 14-cm pupil width and a wavefront error of standard deviation 0.03 waves. Once the perturbation wavefront is formed, it is applied to the complex amplitude distribution in the pupil, the far-field distribution is calculated, and the change in cost function is computed.

Simulated annealing is well known to require extensive computational time. The difficulty of designing phase plates may be characterized by the size of a square computer array (represented as $N \times N$) needed to represent the phase plate. The number of distinct optical modes scales approximately as N^2, and the time per calculation step also scales as N^2. The largest array reported in the literature that has been used for phase-plate design was 128 × 128.[6] For the calculations described in this article, it was necessary to use arrays of 1024 × 1024, leading to an increase in calculation time of nearly four orders of magnitude when compared with studies with the array size 128 × 128.

The literature contains various prescriptions for cooling schedules to achieve optimum or near-optimum performance in a minimum time.[7–9] In most cases the cooling schedules are, at least in part, determined heuristically by numerical experiments for the particular type of problem of interest to the respective authors. To determine the feasibility of the simulated-annealing technique for our application, which includes a very large number of optical modes, we started with a purely cooling or quenching phase (distinct from simulated annealing) in which the temperature T was set to zero; i.e., no reversal steps were allowed. Starting from an unaberrated pupil, we found the process converged in about 2,000 cycles. The minimized cost function resulting from this calculation (S_1) established a benchmark with which to compare the subsequent simulated annealing procedure. We then set the temperature T so that the cost function rose to approximately four to five times S_1 and then cooled exponentially with a time constant of 1,500 cycles for the next 8,000 cycles. This second phase of the procedure is true simulated annealing since reversal steps are allowed, according to the temperature and current cost function. At the end of the simulated annealing phase, the cost function was reduced from its value S_1 at the end of the quenching phase by about a factor of 3. This calculation took about 120 h of CPU time on the Cray YMP-2 at LLE.

Figures 64.25 and 64.26, respectively, show the azimuthally averaged far-field profile for phase plates designed by phase retrieval and simulated annealing. Both designs were done for the same super-Gaussian profile with $M = 8$. Although the simulated annealing design was restricted to a continuous phase-plate surface, it achieved a much better fit to the desired super-Gaussian shape. The phase-retrieval design was well converged in about ten cycles, while the simulated-annealing design required 10,000 cycles. It is possible that other cooling schedules would give faster convergence and lower asymptotic cost functions.

The continuous-surface design has the advantage that it is free of steep surface slopes and discontinuities, resulting in low wide-angle scattering—an advantage not built into the cost function. The effect of wide-angle scattering is seen in Fig. 64.25 by the very slow decay at large radii, in contrast to Fig. 64.26, which shows rapid decay toward zero irradiance at large radii. In practice, the phase-retrieval design would produce more wide-angle scattering than shown in Fig. 64.25. This is because this design leads to steep surface slopes in the vicinity of surface vortices and 2π line discontinuities, which result in about 5%–10% wide-angle scattering. The effect of

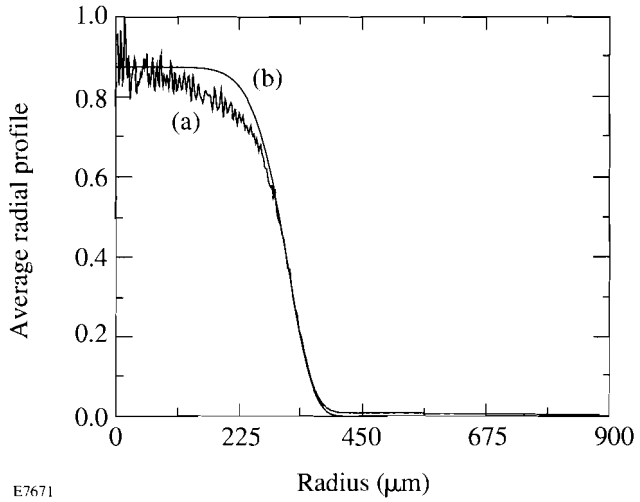

Figure 64.25
Azimuthal average of the far-field irradiance [curve (a)] due to a phase plate designed by the phase-retrieval algorithm, using the parameters defined in the text. The smooth line [curve (b)] is the ideal eighth-order super-Gaussian profile. The azimuthal average provides considerable smoothing of the data, particularly at the larger values of radius. The phase-retrieval solution shows shoulder droop and a rather slow decay to zero at large radius because of wide-angle scattering from steep surface slopes.

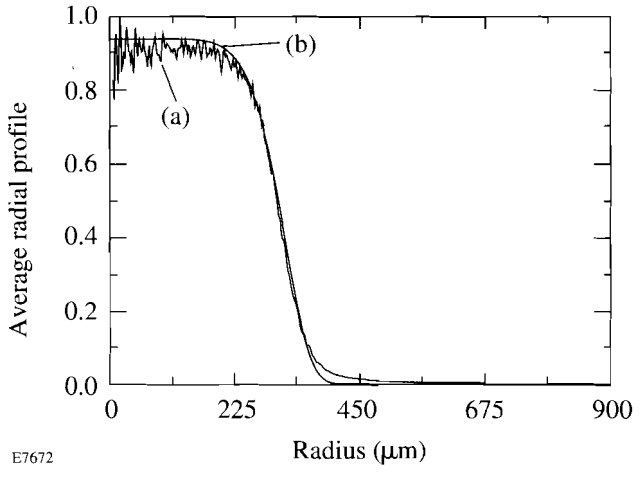

Figure 64.26
Azimuthal average of the far-field irradiance [curve (a)] due to a phase plate designed by the simulated-annealing algorithm. The conditions are the same as for Fig. 64.25, with curve (b) again the ideal profile. The shoulder of curve (a) is considerably more square than for phase retrieval, and the decay to zero is more rapid, indicating little wide-angle scattering because there are no steep surface slopes.

the line discontinuities does not appear in the calculation because the width of the discontinuities is effectively zero, but some finite width will inevitably be present in the manufactured phase plate.

Scans in two orthogonal directions of the target-plane irradiation profile from phase plates generated using the simulated-annealing algorithm are shown in Fig. 64.27. Unlike Figs. 64.25 and 64.26, no azimuthal averaging has taken place. The large (100% rms) modulations seen are characteristic of far-field phase-plate profiles. The small amount of energy loss outside a diameter of 800 μm is evident.

Overlapping Laser Beams

Flat-foil Rayleigh-Taylor instability experiments require a large number of overlapping laser beams to supply the desired irradiance and uniformity. In particular, the lower-order modes of the irradiance pattern must be minimized to allow for uniform foil acceleration and a careful study of the instabilities associated with high-order modes. There are two primary approaches to obtaining a uniform focal plane envelope from a hexagonal set of six beams from the OMEGA system. The first approach involves using the current OMEGA phase plates, which produce weak super-Gaussian profiles, and offsetting the beams in the target plane by an amount chosen to optimize

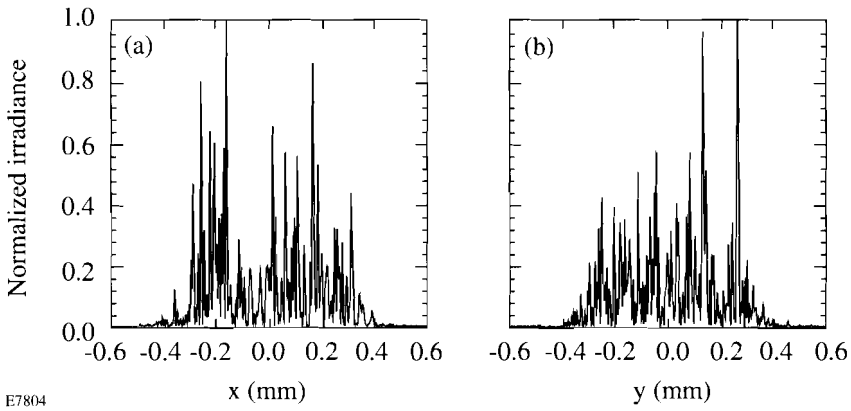

Figure 64.27
Target-plane irradiance profiles resulting from the simulated-annealing algorithm, (a) vertical and (b) horizontal, showing the high modulation speckle that is characteristic of phase converting a laser beam to over 100 times its intrinsic diffraction limit.

the flatness of the envelope. This method represents a compromise between unwanted modulation, energy loss, and envelope uniformity. The second method involves phase converting the laser beams to produce super-Gaussian beam profiles. This method is preferred because it leads to greater energy efficiency and a larger spatial region of uniform irradiation.

The two-dimensional irradiance pattern for six overlapping laser beams, each phase converted with a super-Gaussian phase plate designed by the simulated-annealing algorithm, is shown in Fig. 64.28. In this case the six beams have the same pointing, resulting in a smaller irradiated region than that produced by offsetting the beams radially from the center of the target. This plot shows the time-instantaneous speckle modulation, which is reduced from 100% to 40% due to the uncorrelated (intensity) addition of the six laser beams. The irradiated region is also seen to be circular, as desired. The encircled energy within an 800-μm spot is 97% for this design.

The azimuthally averaged profile of this irradiance distribution is shown as curve (a) in Fig. 64.29. Curve (b) is an eighth-order super-Gaussian profile, which is nearly the same as each individual beam envelope but a little wider because the beams irradiate the target at an angle of incidence of ~20°. Figure 64.30 shows vertical and horizontal cross sections of the six-beam irradiance on target, without azimuthal averaging. Comparing with Fig. 64.27, the modulation of the speckle is reduced from 100% to 40% due to the $\sqrt{6}$ statistical dependence. A certain amount of energy is lost in the wings of the irradiance distribution. Given that the most useful portion of the irradiance distribution is the flat portion in the center, there is a premium on producing the flattest individual profiles possible. These profiles should remain flat under many realizations of the laser-beam phase error. The needs of stability experiments thus provide an impetus for continued phase-plate design at LLE.

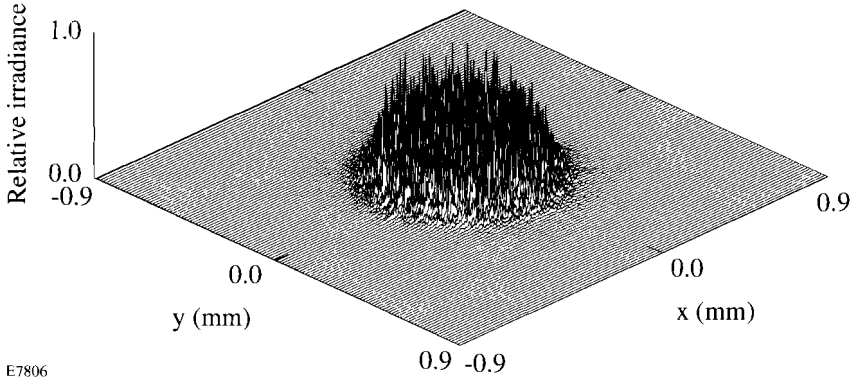

Figure 64.28
Target-plane irradiance pattern for six beams overlapped and focused onto a flat target, each beam phase converted with a super-Gaussian phase plate. The six beams form a hexagonal subset of the 60 OMEGA beams. For flat target irradiation, the speckle modulation is decreased by the square root of the number of overlapped laser beams.

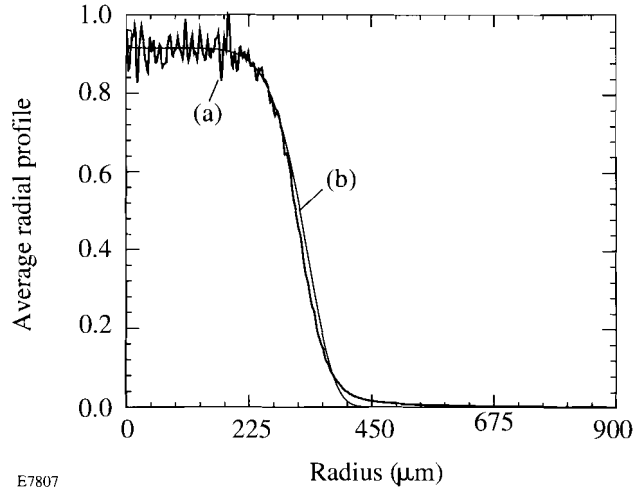

Figure 64.29
Azimuthally averaged profile of the two-dimensional irradiation pattern of Fig. 64.28. It is found that 97% of the energy is contained within an 800-μm-diameter circle. The 500-μm-diameter flat region can be extended by pointing the six beams away from the center of the target.

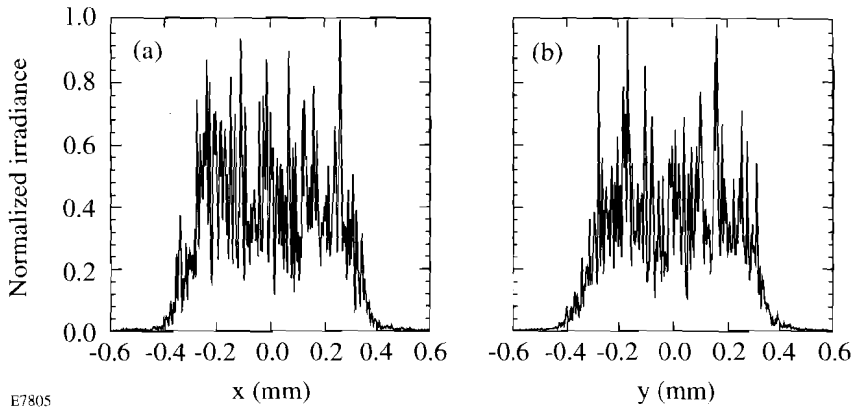

Figure 64.30
Target-plane irradiance profiles, (a) vertical and (b) horizontal, showing a reduction in speckle modulation compared with Fig. 64.27. This is characteristic of overlapping phase-converted laser beams. The contrast of the modulation is reduced from 100% to 40%, which is the expected $\sqrt{6}$ improvement in the time-instantaneous uniformity.

Summary

A simulated annealing algorithm has been developed to design distributed phase plates that produce super-Gaussian irradiance profiles. This approach uses a strictly continuous surface relief that minimizes wide-angle scattering. Phase plates produced using this algorithm perform better than those produced using the previous phase-retrieval algorithm, which suffer from steep surface slopes and line discontinuities. The new algorithm also allows great flexibility in defining the cost function and constraints to meet the requirements of the target experiments to be performed.

Super-Gaussian phase plates can be fabricated and used to conduct experiments involving multiple overlapping beams. This is important for studies of the Rayleigh-Taylor instability on flat targets. In addition to enhancing the energy efficiency, the simulated-annealing technique offers the capability of controlling the power spectrum of the individual beams used to irradiate targets.

Future work will involve reducing the computation time for the algorithm, decreasing the sensitivity of the phase-plate performance to the laser-beam phase errors, and gaining greater control of the power spectrum placed on target.

ACKNOWLEDGMENT

This work was supported by the U.S. Department of Energy Office of Inertial Confinement Fusion under Cooperative Agreement No. DE-FC03-92SF19460, the University of Rochester, and the New York State Energy Research and Development Authority. The support of DOE does not constitute an endorsement by DOE of the views expressed in this article.

REFERENCES

1. S. N. Dixit *et al.*, Opt. Lett. **19**, 417 (1994).
2. Y. Lin, T. J. Kessler, and G. N. Lawrence, Opt. Lett. **20**, 764 (1995).
3. Laboratory for Laser Energetics LLE Review **63**, NTIS document No. DOE/SF/19460-91, 1995 (unpublished), p. 126.
4. S. Kirkpatrick, C. D. Gelatt, Jr., and M. P. Vecchi, Science **220**, 671 (1983).
5. S. Kirkpatrick, J. Stat. Phys. **34**, 975 (1984).
6. S. Yin, M. Lu, C. Chen, F. T. S. Yu, T. D. Hudson, and D. K. McMillen, Opt. Lett. **20**, 1409 (1995).
7. H. Szu and R. Hartley, Phys. Lett. A **122**, 157 (1987).
8. N. Yoshikawa and T. Yatagai, Appl. Opt. **33**, 863 (1994).
9. K. Ergenzinger, K. H. Hoffman, and P. Salamon, J. Appl. Phys. **77**, 5501 (1995).